TRANSPORT PROBLEMS 2022 Volume 17 Issue 3
PROBLEMY TRANSPORTU DOI: 10.20858/tp.2022.17.3.01

Keywords: simulation; Matlab; crane; dynamics; spring pendulum

Tomasz HANISZEWSKI[1]*, Jerzy MARGIELEWICZ[2], Damian GĄSKA[3], Tadeusz OPASIAK[4]

NEW CRANE BUMPER DESIGN WITH AN ENERGY ABSORPTION DEVICE SYSTEM

Summary. This article presents research carried out using physical data from the experimental construction of an overhead crane. This article aims to determine the dynamic behaviour of the cart-pendulum system when the hoisting mechanism hits the new bumper design at the end of the girder support structure with selected speed and bumper material to the length of the wire rope. This research shows the influence of the horizontal speed of the hoisting mechanism on the bumper force during a collision with a standard buffer and its modifications. The presented model can be the basis for modelling more complex cases, and its assumed role (i.e. the ability to determine the angle of deflection of the rope during an impact) has been confirmed and is possible to use in a specific case of an overhead crane on an industrial scale. Preliminary analysis of the construction of the bumper considered reveals its positive features, aiming, among other goals, to reduce the acceleration and force acting on the crane cart in emergency situations.

1. INTRODUCTION

Cranes are one of the most widely used devices in the industry sector, performing tasks involved in transporting cargo from one place to another. A characteristic feature of these machines is the intermittent nature of the work cycle and the need to perform hundreds of thousands of cycles during the machine's life. For this reason, knowledge of the dynamics of load movement and transport plays a significant role in the context of positioning and control of mechanisms and loads involving the load-carrying and supporting structure. Overhead cranes are used in production plants, landfills, halls and warehouses and in the transport processes of various machine components and bulk and unitized goods over short distances. Because they work above the storage and/or production area, they are a great alternative to, for example, forklift trucks [1, 2].

A crane bumper (or industrial buffer) is a device installed to absorb the energy of a moving crane, thereby protecting the crane, the building in which it may operate and personnel in the immediate area from damage caused by impact with other cranes or end stops on the track. Today crane bumpers are divided into two types: energy-consuming bumpers – mainly hydraulic bumpers (Figs. 1a–c) but also those made of composites and polyurethane (Fig. 1d) – and storage type bumpers (spring bumpers and rubber bumpers). There has been rapid development in hydraulic bumpers (Figs. 1a–c) with capacities and lengths to meet the demands of increasing crane weights and speeds. When the hydraulic bumper is subjected to an impact pressure, the kinetic energy is transferred to the piston by the plug and the

[1] Silesian University of Technology, Faculty of Transport and Aviation Engineering; Krasińskiego 8, 40-019 Katowice, Poland; e-mail: tomasz.haniszewski@polsl.pl; orcid.org/0000-0002-4241-6974
[2] Silesian University of Technology, Faculty of Transport and Aviation Engineering; Krasińskiego 8, 40-019 Katowice, Poland; e-mail: jerzy.margielewicz@polsl.pl; orcid.org/0000-0003-2249-4059
[3] Silesian University of Technology, Faculty of Transport and Aviation Engineering; Krasińskiego 8, 40-019 Katowice, Poland; e-mail: damian.gaska@polsl.pl; orcid.org/0000-0002-2968-1626
[4] Silesian University of Technology, Faculty of Transport and Aviation Engineering; Krasińskiego 8, 40-019 Katowice, Poland; e-mail: tadeusz.opasiak@polsl.pl; orcid.org/0000-0002-0777-2316
* Corresponding author. E-mail: tomasz.haniszewski@polsl.pl

accelerating spring. The bumper working case is equipped with a spring, piston, cylinder and oil. The movement of the piston squeezes the oil in the working case so that it pushes the spring to compress and squeeze the oil from the annular gap into the reservoir. When a crane with a spring bumper hits an obstacle, the impact energy is converted to the spring compression energy. A similar situation applies to the rubber bumper.

According to [3], when calculating the bumper forces, the effects of suspended loads that are horizontally unrestrained (free to swing) should be considered. However, when the crane speed is reduced before a collision with the buffers, the load may sway forward with the compression of the bumpers. In this case, the mass of the load and the braking deceleration before hitting the bumper (as well as on impact) should be taken into account as an additional horizontal force. The buffer/bumper forces shall be calculated considering the distribution of relevant masses and the bumper's characteristics [4, 5] (mainly the construction and material that affect the principle of operation and, most importantly, the characteristics of a given bumper). Regarding non-linear characteristics, the design, modelling and measurement tasks are difficult. However, such characteristics give better results by compensating the impact energy more effectively than bumpers with a linear characteristic [6].

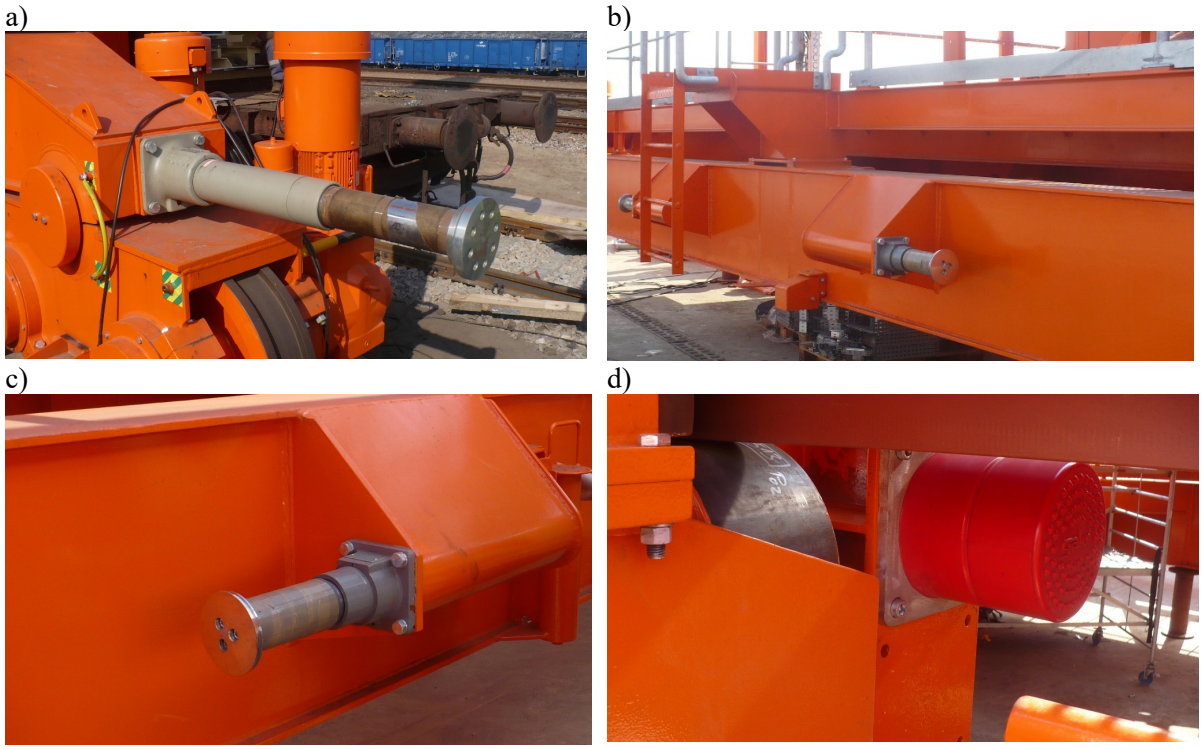

Fig. 1. Types of bumpers mounted on a crane structure: a) a hydraulic bumper on a crane structure, b) and c) a hydraulic bumper on a hoisting winch structure and d) a plastic bumper

Currently, many models addressing the cart-pendulum problem have been presented in the literature, but there is a lack of literature on the cart-pendulum problem with elastic rope type in analysis situations when a crane hits the bumper, especially with different kinds of unusual constructions of energy absorption devices (EADs). This gap is critical in terms of crane dynamics and load positioning [7]. Aguiar et al. [8] proposed a model to assist in the design of a fuzzy controller based on the concept of parallel compensation. The solution guarantees closed-loop Lyapunov stability, bounded control inputs, quick positioning of the supporting cart and suppression of load oscillations and collisions. In [9] an output feedback controller was proposed for the stabilization of the inverted pendulum on a cart in the presence of uncertainties. It has a multi-time-scale structure that allows independent analysis of the dynamics in each time scale, and singular perturbation methods were effectively utilized to establish exponential stability of the equilibrium. Similar anti-swing control methods were proposed in [10] and for the double pendulum crane in [11]. Two control techniques were analyzed in [12].

In this paper, a sliding mode controller to stabilize the pendulum and a state feedback controller to keep the pendulum upright and handle disturbances up to a certain point are proposed. Analysis of controlling and Lyapunov-based design methods for the variable length pendulum, which simulates the hoisting of the crane load, was presented in [13]. Similarly, a methodology for designing controllers that attenuate the payload swing angle in two-dimensional overhead crane systems with varying rope lengths was proposed in [14].

In some situations, the speed control system or limit switches simply do not work or do not work properly. Then, there is a high risk that the cart will hit the bumper with a proportionately large force, depending on the value of the speed at the time of impact and friction in the wheel-rail contact. Additionally, other impact forces occur during the use of cranes (e.g. loads caused by skew) [15]. Another threat is that of several cranes on the same track. Not only must these cranes be properly steered to increase efficiency, but the possibility of their collision must also be anticipated [16, 17]. Therefore, it is important for such large machines to minimize the impact of dynamic forces on the structure or completely eliminate them [18]. In a previous paper [19], a multisensor-driven real-time crane monitoring system was presented consisting of load tracking, obstacle detection, worker detection, collision warning and 3D visualization modules. Such research provides important findings in terms of the challenges and limitations of implementing a crane monitoring system. However, despite advanced control systems, any electronic system is unreliable. Failure of control systems can cause considerable damage to property and threaten lives [20, 21]. Hence, appropriate buffers, as purely mechanical devices, minimize the impact of dynamics on structures [22].

The purpose of this article is to present a phenomenological model that allows the simulation of the impact of the crane cart on the bumper, assuming that the rope is elastic, with or without damping properties.

2. TEST OBJECT

The proposed test object is an overhead travelling crane with a total capacity of 5000 kg. Table 1 shows the general characteristics of the considered overhead crane, and Fig. 1 shows the construction under discussion. As shown in Fig. 1, there is a cart pendulum system connected in a series with a rubber buffer system. In the model under consideration, the buffer, its steel construction and the cart with a load on a rope were taken into account. The buffer includes two parts. The first is steel construction with a mass of 47 kg and a rubber buffer 010 DZg with a mass of 1.5 kg. For further calculations of impact, the velocity of the cart (crane winch) was assumed to be 0.6 m/s, which is the maximum speed of the crane winch of the structure under consideration.

Table 1

Characteristics of the experimental crane

Description		Symbol	Dimension	Value
Lifting capacity		Q	[t]	5
Span		L	[m]	20
Lifting height		$H_{p\,max}$	[m]	16
Operating speed	Lifting	v_h	[m/s]	0.208
	Winch driving	v_j	[m/s]	0.600
Maximum impact force at the bumper at $0.5V_j$		Z_u	N	30e3
Braking distance at $0.5V_j$		S_h	m	0.52

The main purpose of this article is to study the dynamic behaviour of the car-elastic-pendulum system when it hits the buffer at the end of the girder at a selected speed. The results indicate the influence of energy-absorbing systems of the cart-elastic-pendulum (CEP) on the cart deceleration and bumper force to the angle of deflection of rope with a given load. For analysis, a type of buffer made of rubber was selected for testing. The data of the materials used are shown in Table 2.

Based on the geometric model presented in Fig. 2, the numerical finite element model was built using Autodesk Inventor software [24]. The model was loaded with a static force, and the stiffness of the tested bumper was determined based on the deflection. Its dissipation factor value was defined using a Rayleigh proportional damping model. Specified values will be used in further analysis to determine the dynamic behaviour of the cart-pendulum system.

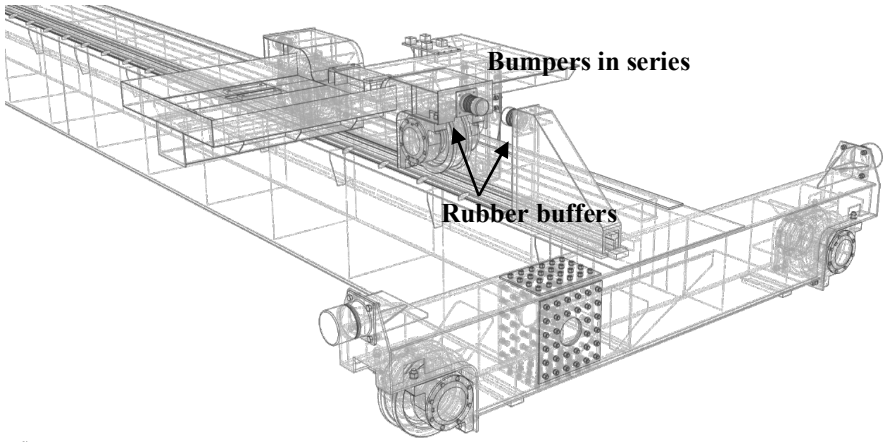

Fig. 2. Considered test object of a crane

Table 2

Material data

Rubber bumper material properties		
Density	ρ	1.25 [g/cm^3]
Poisson's coefficient	ν	0.49 [-]
Young's modulus	E	0.003 [GPa]

3. PHENOMENOLOGICAL MODEL OF A RESEARCH OBJECT

The subject of research presented in this part of the article is a CEP system with and without an EAD, whose mathematical models can be used to simulate the movement of the hoist load of the overhead-travelling crane. Concerning the research topic described in the introduction to this article, Fig. 3 presents the phenomenological model of a cart moving horizontally, equipped with a pendulum with an elastic wire rope without damping. The physical data of the model considered are presented in Table 3.

In Fig. 2, the CEP system without an EAD is presented, where mass m is a hoist load, which relates to elastic wire rope with stiffness, c_l, and m_w is the mass of the cart. Damping factor b is included in the model to consider the influence of friction between the wire rope and rope drum. The parameters b_1 and c_1 (and c_2, b_2) parameters are included for the simulation of rubber buffer damping and stiffness. The second part of the phenomenological model is an inverted physical pendulum, which represents a steel construction of a buffer holder (Fig. 2), where h_{zd} is the height of its construction, m_{zd} is its mass and b_{zd} and c_{zd} are the rotational damping and stiffness of the buffer holder construction.

Considering the simulation of a collision with the buffer, the dynamic model (Fig. 3) has been created by adding a model of the collision by using a gap δ, which is presented in Equations (2-6).

The model was based on the concept of generalized coordinates and the phenomenological model presented in Fig. 3 after applying the second kind of Lagrange equation (1):

$$\frac{d}{dt}\left(\frac{\partial E_k}{\partial \dot{q}_j}\right) - \frac{\partial E_k}{\partial q_j} + \frac{\partial E_p}{\partial q_j} + \frac{\partial E_R}{\partial \dot{q}_j} = F_j, j = 1,2,\dots,n \tag{1}$$

where: t - time [s]; q_j - generalized displacement [m]; $\dot{q}_j$ - generalized speed [m/s]; n - number of degrees of freedom [-]; F_j - generalized force [N]; E_k - kinetic energy [J]; E_p - potential energy [J]; E_R - dissipation function [J/s].

Table 3

Physical parameters describing the dynamic system

No	Symbol	Value	Dimension	No	Symbol		Value	Dimension
1	m	1800	kg	14		b	1e3	Ns/m
2	m_w	2020	kg	15		h_{zd}	0.585	m
3	m_z	47	kg	16		c_{zd}	40.5e6	Nm/rad
4	v_j	0.6	m/s	17		b_{zd}	8.3e4	Nms/rad
5	d_{wire_rope}	12e-3	m	18	8 m	c_l	6.53e6	N/m
6	g	9.81	m/s^2	19	8 m	b_l	3.2640e4	Ns/m
7	μ	0.05	-	20	2 m	c_l	2.61e7	N/m
8	μ_e	0.05	-	21	2 m	b_l	1.3056e5	Ns/m
9	l	2, 8	m	22		c_z	8.5e5	N/m
10	J_{zd}	5.36	kgm^2	23		b_z	1.7e3	Ns/m
11	c_e	2.5e4	N/m			b_e	1e3	Ns/m
12	m_e	500	kg					
13	δ	1	m					

Dynamic motion equations were formulated (3). In the model under consideration, the velocity of mass m suspended on the rope is given by the following equation:

$$V_c^2 = (y^2 + 2ly + l^2)\left(\frac{d\Theta}{dt}\right)^2 + 2(y+l)\left(\frac{dx_q}{dt}\right)\cos(\Theta)\left(\frac{d\Theta}{dt}\right) + 2\left(\frac{dx_q}{dt}\right)\left(\frac{dy}{dt}\right)\sin(\Theta) + \left(\frac{dy}{dt}\right)^2 + \left(\frac{dx_q}{dt}\right)^2 \quad (2)$$

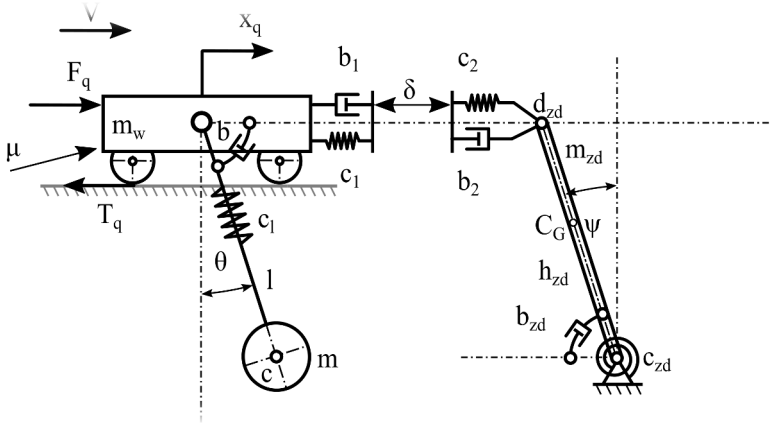

Fig. 3. Phenomenological model of the considered cart pendulum system with a standard bumper

Considering the relevant functions' defining excitations, the system of four non-linear differential equations shown below was obtained:

$$\begin{gathered}
(y+l)^2\left(\frac{d^2\Theta}{dt^2}\right) + 2(y+l)\left(\frac{dy}{dt}\right)\left(\frac{d\Theta}{dt}\right) + \frac{b}{m}\left(\frac{d\Theta}{dt}\right) + gl\,sin(\Theta) + (y+l)\left(\frac{d^2x_q}{dt^2}\right)cos(\Theta) = F_q \\
\left(\frac{d^2y}{dt^2}\right) + \frac{c_l}{m}y - (y+l)\left(\frac{d\Theta}{dt}\right)^2 + \left(\frac{d^2x_q}{dt^2}\right)sin(\Theta) = 0 \\
(m_w+m)\left(\frac{d^2x_q}{dt^2}\right) + m(y+l)\cos\Theta\left(\frac{d^2\Theta}{dt^2}\right) - m(y+l)\,sin(\Theta)\left(\frac{d\Theta}{dt}\right)^2 + 2m\left(\frac{dy}{dt}\right)\left(\frac{d\Theta}{dt}\right)cos(\Theta) \\
+ m\left(\frac{d^2y}{dt^2}\right)sin(\Theta) = -T_q + F_z
\end{gathered} \quad (3)$$

$$\frac{{h_{zd}}^2 m_{zd}}{3}\left(\frac{d^2\psi}{dt^2}\right) + b_{zd1}\left(\frac{d\psi}{dt}\right) + c_{zd1}\psi - gh_{zd}m_{zd}\,sin(\psi) = -h_{zd}F_z$$

where bumper force is described as

$$F_z = \begin{cases} 0, & |\xi| \le \delta \\ c_z\big(\xi - \delta sgn(\xi)\big) + b_z\left(\frac{d\big(\xi - \delta sgn(\xi)\big)}{dt}\right), & |\xi| > \delta \end{cases}$$
$$\xi = h_{zd}\psi - x_q \tag{4}$$
$$c_z = \frac{c_1 c_2}{c_1 + c_2}, b_z = \frac{b_1 b_2}{b_1 + b_2}$$

Moreover, T_q is the sliding friction between the surface of the cart and the rail. This parameter was considered assuming only its kinetic value in the model; more complex friction models like in [23] are recommended for future simulations.

$$T_q = \mu g(m_w + m) sign\left(\frac{dx_q}{dt}\right) \tag{5}$$

The second model presented in Fig. 4 had a modified bumper construction. In this case, the bumper construction was supported on a frictionless base with a connection to an EAD. Based on the model presented in Fig. 4, dynamic motion equations were formulated as follows. In this model, the damping of the wire rope was added and denoted as a parameter b_l.

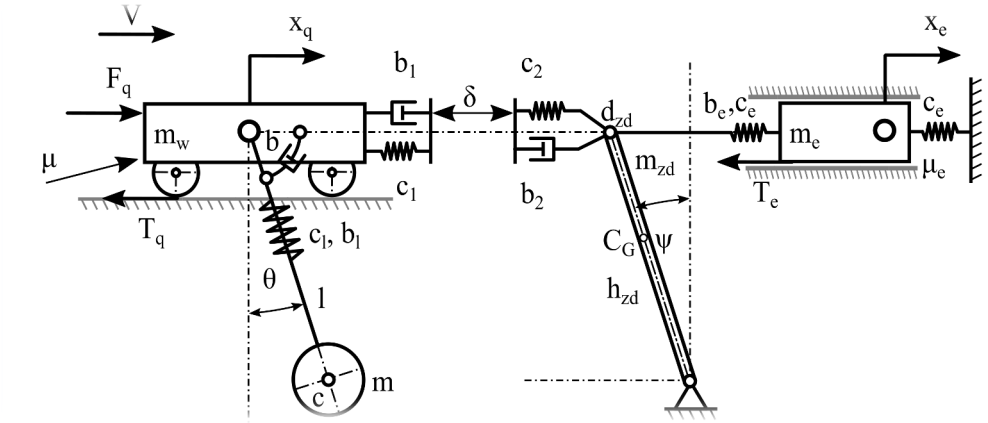

Fig. 4. The phenomenological model of the considered cart pendulum system with modified bumper

$$(y+l)^2\left(\frac{d^2\Theta}{dt^2}\right) + 2(y+l)\left(\frac{dy}{dt}\right)\left(\frac{d\Theta}{dt}\right) + \frac{b}{m}\left(\frac{d\Theta}{dt}\right) + gl\,sin(\Theta) + (y+l)\left(\frac{d^2x_q}{dt^2}\right)cos(\Theta) = F_q$$
$$\left(\frac{d^2y}{dt^2}\right) + \frac{c_l}{m}y - (y+l)\left(\frac{d\Theta}{dt}\right)^2 + \left(\frac{d^2x_q}{dt^2}\right)sin(\Theta) + b_l\left(\frac{dy}{dt}\right) = 0$$
$$(m_w + m)\left(\frac{d^2x_q}{dt^2}\right) + m(y+l)\,cos\,\Theta\left(\frac{d^2\Theta}{dt^2}\right) - m(y+l)\,sin(\Theta)\left(\frac{d\Theta}{dt}\right)^2 + 2m\left(\frac{dy}{dt}\right)\left(\frac{d\Theta}{dt}\right)cos(\Theta) + \tag{6}$$
$$+m\left(\frac{d^2y}{dt^2}\right)sin(\Theta) = -T_q + F_z$$
$$\frac{{h_{zd}}^2 m_{zd}}{3}\left(\frac{d^2\psi}{dt^2}\right) - gh_{zd}m_{zd}\,sin(\psi) + c_e h_{zd}(h_{zd}\psi - x_e) = -h_{zd}F_z$$
$$m_e\left(\frac{d^2x_e}{dt^2}\right) - c_e(h_{zd}\psi - x_e) - b_e\big(h_{zd}\dot{\psi} - \dot{x_e}\big) + c_e x_e = -\mu_e g m_e sign\left(\frac{dx_e}{dt}\right)$$

The obtained system of motion equations is inertia coupled. The model built directly on their basis (i.e. the Matlab\Simulink model) contained algebraic loops on the signal lines representing the second derivatives of generalized coordinates. The standard way to solve the problem of algebraic loops is to

break them with the signal delay element. Doing this, however, affect the accuracy of numerical calculations. The delay signal is a sort of extra damping in the system, which, in this case, is difficult to physically justify. Due to the accuracy of numerical calculations, the inertial decoupling of the system of motion equations is advisable.

4. SIMULATION RESULTS

The research plan included carrying out a series of simulations of the proposed models. Two different lengths of the wire rope were considered, modelling a situation where the brakes do not work at all and the cart hits the buffer with the full assumed speed, which in this case is $0.6\ m/s$. The control unit shown in Fig. 5 was used to achieve the effect of driving the cart from starting up to turning off the drive through the limit switch without the influence of the braking system.

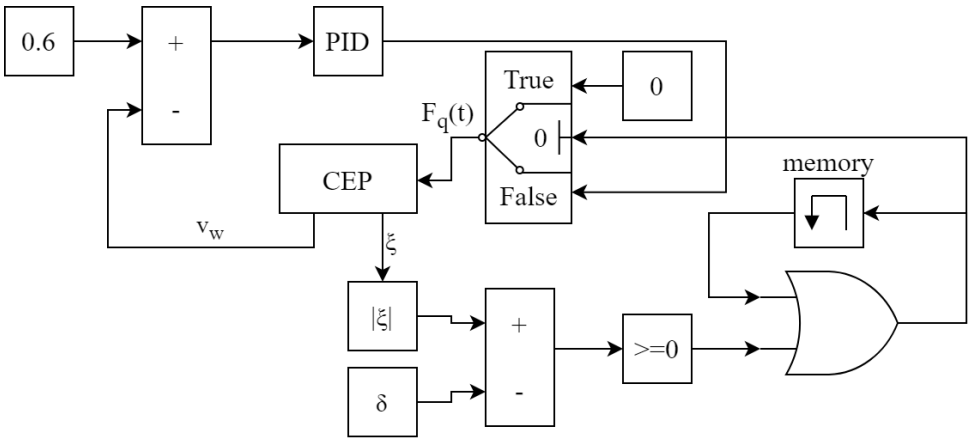

Fig. 5. Force $F_q(t)$ control system

The control system was based on a PID controller and several conditions related to the current distance of the cart from the bumper and the set value of this gap. The system generates a force $F_q\ (t)$, causing the crane cart to accelerate to $0.6\ m/s$. Then, when the cart's buffers and the bumper come into contact (i.e. when the limit switch is turned on), the drive is disengaged but without the braking force. This experiment aimed to verify an emergency that may occur in the event of the operation of cranes.

Every simulation included two variants: VAR A involved a CEP system without an EAD, and VAR B involved a CEP system with an EAD.

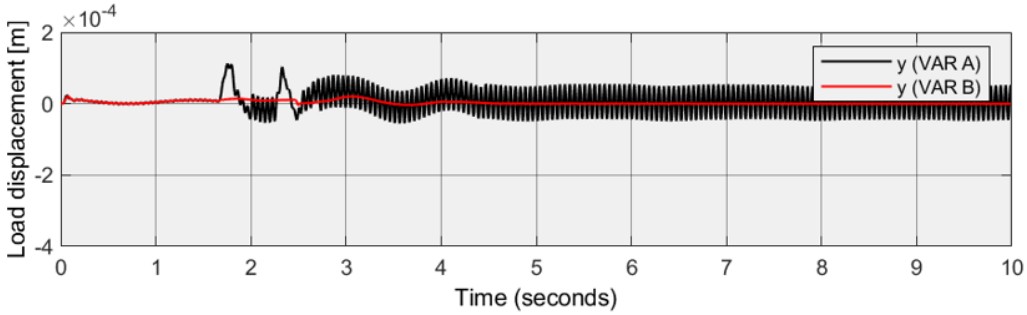

Fig. 6. Oscillogram of the rope elongation for L=2 m

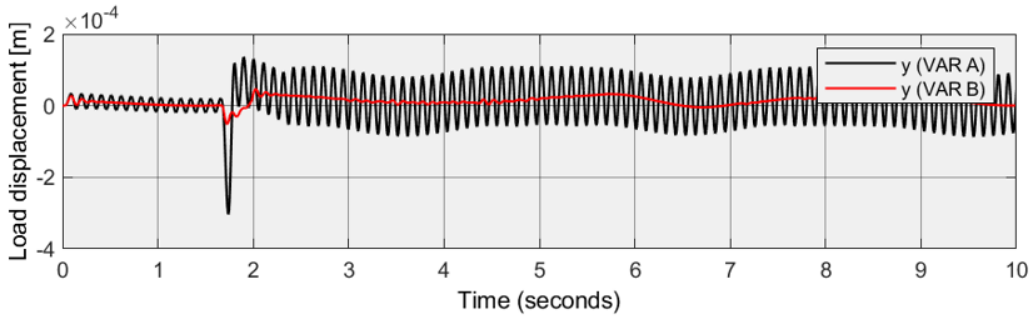

Fig. 7. Oscillogram of the rope elongation for L=8 m

The system was forced by $F_q(t)$ in the initial phase of the start-up of the cart. The cart movement was simulated at the set value of force and the distance between the cart and the bumper so that the cart's speed at the impact was 0.6 m/s. Figs. 6–17 present selected results of the simulations.

Figures 6 and 7 show the difference between the oscillation of vertical movement of the load. The values are mainly connected with the damping properties of the rope that was added to the second model and the EAD system (Figs. 6 and 7; VAR B – system with an EAD).

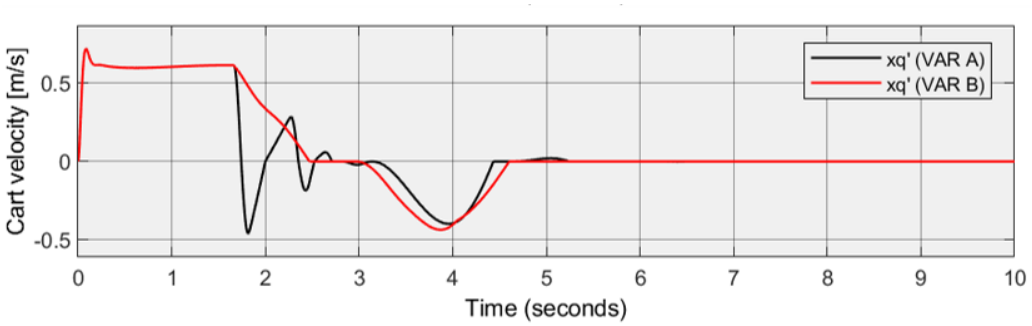

Fig. 8. Cart speed oscillogram for L=2 m

The amount of elongation is related to the basic length of the rope. As can be seen, at the moment of collision (1.8 s from start-up; Figs. 8 and 9), there was a rapid increase in the amplitude of vertical vibrations of the load suspended on a flexible wire rope. As can be seen in Fig. 7, the effect of the rapid deceleration of velocity (Figs. 8 and 9) associated with hitting a high-stiffness bumper induced a much greater increase in the vibration amplitude compared to the VAR B variant, where the effect of increasing vertical vibrations was reduced using the EAD absorber system. This effect was intensified by the considerable length of the wire rope (which reduced the rope's stiffness). The reduction of the vibration amplitude can also be seen in Fig. 6 for the 2-m-long rope.

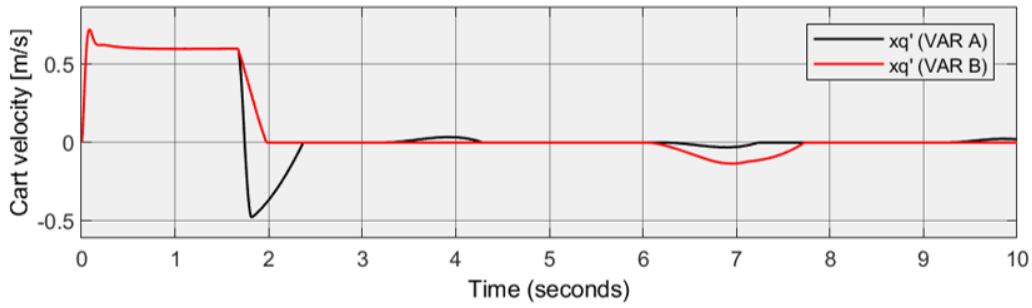

Fig. 9. Cart speed oscillogram for L=8 m

Observed values and the length of the rope $l = 8\,m$ had a maximum of $2.99e-4\,m$ for VAR A and $5.14e-5\,m$. A similar situation occurred for the system with a 2-m-long rope; for VAR A, the

maximum value was $1.03e-4\ m$, and for VAR B, it was $2.07e-5\ m$, which gives a reduction of vertical vibrations by 480% for a rope with a length of $8\ m$ for the variant with the EAD system, and a reduction of 400% for the system with a rope length of $2\ m$.

As can be seen in Figs. 8 and 9, the impact velocity was $0.6\ m/s$, which caused the rope to be deflected by $14\ deg$ for a 2-m-long rope (Fig. 10) and $5.7\ deg$ for an 8-m-long wire rope (Fig. 11). As can be seen for a short section of the rope (i.e. a load suspended at a high height), the use of the EAD system made it possible to reduce load swing (Fig. 10) by 40.5% when hitting a buffer.

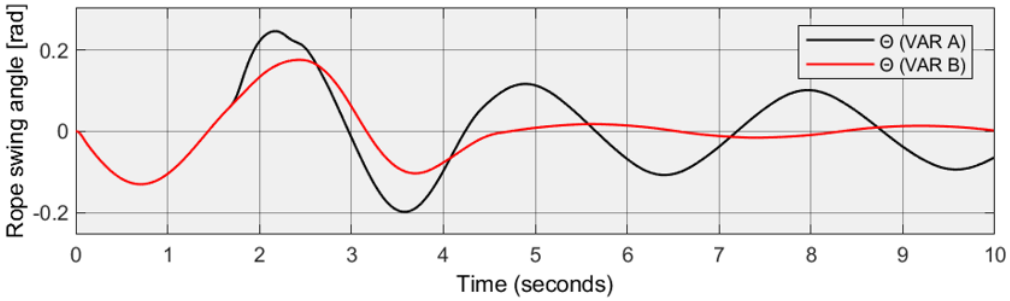

Fig. 10. Oscillogram of the angular displacement of the mass on the rope for L=2 m

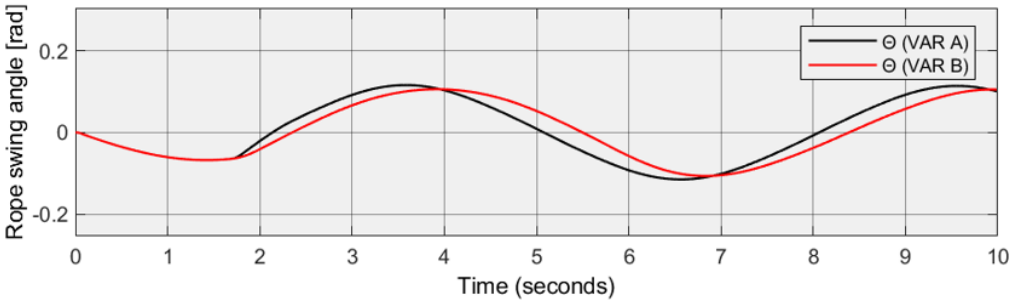

Fig. 11. Oscillogram of the angular displacement of the mass on the rope for L=8 m

Figs. 8 and 9 also show that the model with the EAD system caused a mild loss of speed (1–2 seconds of simulation) to the sudden stop in the case of the system with a traditional buffer. Naturally, this significantly impacted the values of accelerations and decelerations, thereby affecting the components of the crane cart.

Figs. 12 and 13 show the oscillograms showing the changes in accelerations and decelerations for the tested systems. As can be seen in both cases (i.e. regardless of the length of the rope), the use of the EAD system allows for an almost seven-fold reduction in deceleration at the moment of collision.

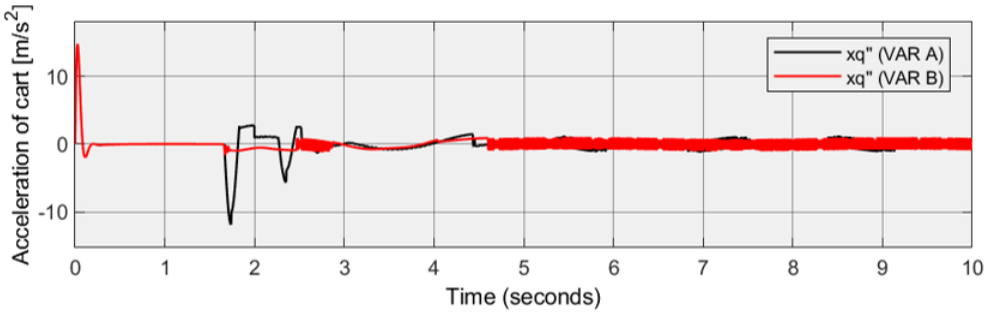

Fig. 12. Cart acceleration oscillogram for L=2 m

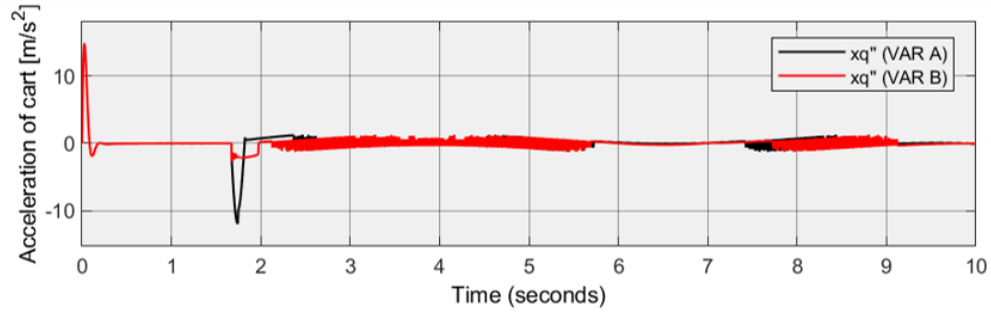

Fig. 13. Cart acceleration oscillogram for L=8 m

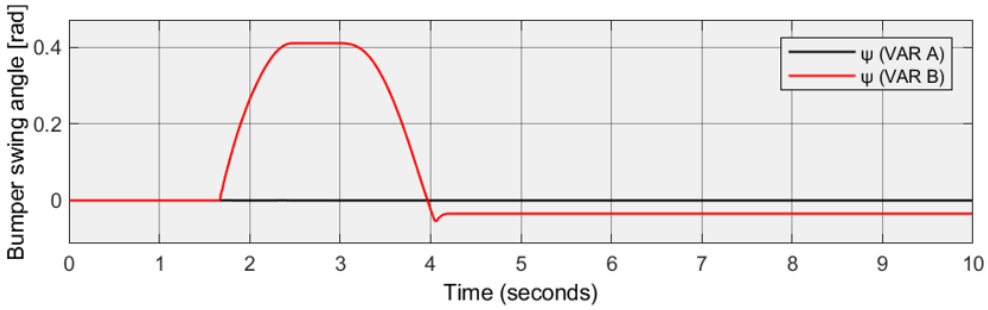

Fig. 14. Oscillogram of the angular displacement of the bumper support structure for L=2 m

In connection with the torsional use of a flexible bumper, it will naturally deviate from the equilibrium position, as shown in Figs. 14 and 15. It should be well known that the values obtained are highly controllable depending on the necessary values of both the angle of maximum deflection of the bumper and the reduction of acceleration by selecting the mass, m_e, the elastic damping parameters, c_e, b_e, and the friction coefficient, μ_e.

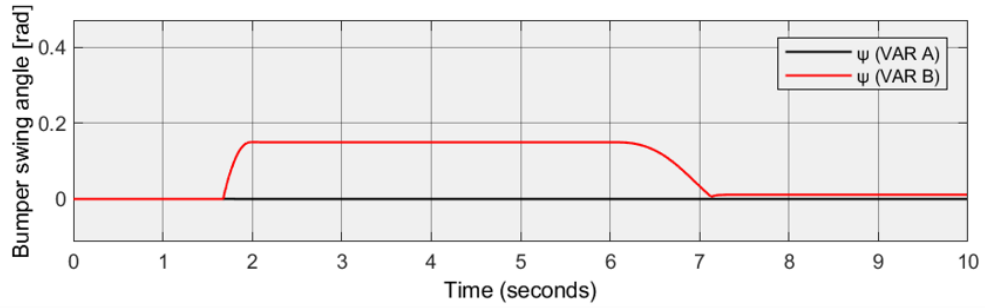

Fig. 15. Oscillogram of the angular displacement of the bumper support structure for L=8 m

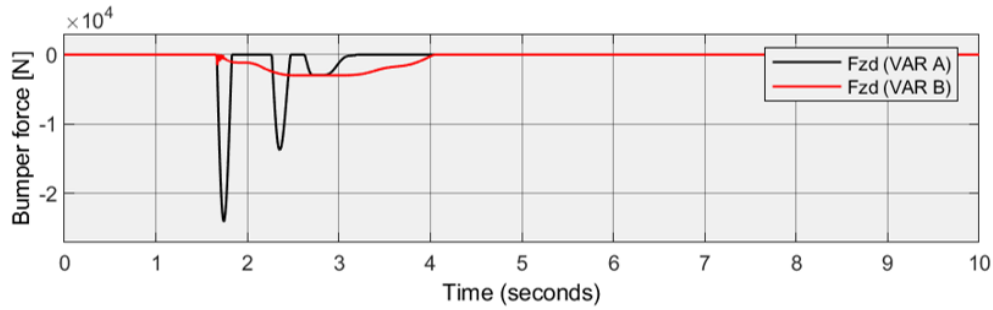

Fig. 16. Impact force oscillogram for L=2 m

As depicted in Figs. 16 and 17, the impact force had values of $2.4e4\ N$ for $l = 2\ m$ and $2.13e4\ N$ for $l = 8\ m$ for VAR A, which is the standard construction of a buffer. These values were $2.99e3\ N$ for $l = 2\ m$ and $1.4e3\ N$ for $l = 8\ m$ for the second model proposed in this article with an EAD system.

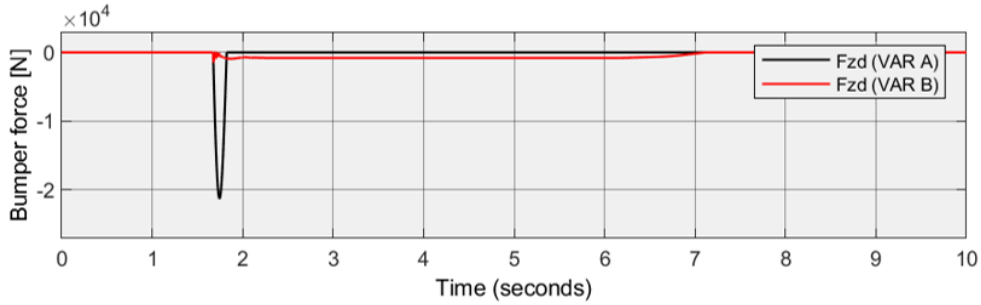

Fig. 17. Impact force oscillogram for L=8 m

The new construction yields about seven times less impact force for a 2-m-long rope and 14 times less impact for an 8-m-long wire rope. In this case, the acceleration of the cart was naturally smaller, yielding a nearly seven-fold decrease in the acceleration of moving masses (Figs. 16 and 17).

5. CONCLUSIONS

This article presents a model that allows the simulation of a collision of a crane cart with a bumper at the selected speed. The presented systems expressed in Equations (3) and (6) are inertially coupled. Therefore, the direct determination of time courses of the tested signals was impossible due to the occurrence of algebraic loops. Matlab/Simulink software offers a function to overcome this problem using delays of the signal in the loop. Using a sufficiently small-time step, the problem of artificial damping of the vibrations of the system, which has no physical justification, can be eliminated. The proposed system of equations was not decoupled because the test simulations were only preliminary. The proposed solution in the form of an EAD system for reducing forces and accelerations of the cart-pendulum system in the crane has not been optimized in terms of parameter values. Hence, the values of forces, angular displacements of the load and delays of the crane trolley did not necessarily reach the minimum values. The selection of optimal parameters could significantly increase the efficiency of the proposed EAD system, which is the purpose of further research on the discussed system.

Despite the use of basic methods to select these parameters, the obtained results of the simulation tests are promising, especially in terms of the reduction of cart decelerations and the forces at the contact of the buffer system. For example, for the considered parameters, the vertical vibrations were reduced by 480% for a rope with a length of 8 m for the variant with the proposed EAD system. Further, the use of the EAD system reduced load swing by 40.5% when the crane winch hit the buffer.

The presented model can be the basis for modelling more complex cases, and its assumed role (i.e. the ability to determine the angle of deflection of the rope during an impact) has been confirmed and can be used in a specific case of an overhead crane on an industrial scale. Preliminary analysis of the construction of the bumper considered reveals its positive features, which aimed, among other goals, to reduce the acceleration and force acting on the crane cart in emergency situations.

References

1. Gąska, D. *Model research of load – carrying crane structures and hoist load dynamics in the context of regular and chaotic vibrations*. Wydawnictwo Politechniki Śląskiej. Gliwice, 2019.
2. Haniszewski, T. *Metodyka modelowania mechanizmów wykonawczych suwnic*. Wydawnictwo Politechniki Śląskiej. Gliwice 2021.
3. EN 13001-2:2020. *Crane safety - General design - Part 2: Load actions*.
4. Haniszewski, T. Modeling the dynamics of cargo lifting process by overhead crane for dynamic overload factor estimation. *J. Vibroeng*. 2017. Vol. 19. No. 1. P. 75-86.

5. Stańco, M., & Działak, P. & Żędzianowski, B. Numerical and experimental analysis of the rubber bumper stiffness. *Materials Today: Proceedings.* 2019. Vol. 12. P. 508-513.
6. Haniszewski, T. Preliminary modeling studies of sudden release of a part of the hoist load with using experimental miniature test crane. In: *Vibroengineering Procedia*. 2017. Vol. 13.
7. Beller, S. & Yavuz, H. Crane automation and mechanical damping methods. *Alexandria Engineering Journal.* 2021. Vol. 60. P. 3275-3293.
8. Aguiar, C. & Leite, D. & Pereira, D. & Andonovski, G. & Škrjanc, I. Nonlinear modeling and robust LMI fuzzy control of overhead crane systems. *Journal of the Franklin Institute*. 2021. Vol. 358. P. 1376-1402.
9. Lee, J. & Mukherjee, R. & Khalil, H.K. Output feedback stabilization of inverted pendulum on a cart in the presence of uncertainties. *Automatica.* 2015. Vol. 54. P. 146-157.
10. Maghsoudi, M. & Mohamed, A. & Sudin, S. & Buyamin, S. & Jaafar, H.I. & Ahmad S.M. An improved input shaping design for an efficient sway control of a nonlinear 3D overhead crane with friction. *Mechanical Systems and Signal Processing.* 2017. Vol. 92. P. 364-378.
11. Wu, Q. & Wang, X. & Hua, L. & Xia, M. Dynamic analysis and time optimal anti-swing control of double pendulum bridge crane with distributed mass beams. *Mechanical Systems and Signal Processing.* 2020. Vol. 144. No. 106968.
12. Mathew, N.J. & Rao, K.K. & Sivakumaran, N. Swing up and stabilization control of a rotary inverted pendulum. 2013. In: *IFAC Proceedings Volumes (IFAC-PapersOnline)*. 2013. Vol. 10. IFAC.
13. Anderle, M. & Appeltans, P. & Celikovskýet, S. & et al. Controlling the variable length pendulum: Analysis and Lyapunov based design methods. *Journal of the Franklin Institute.* 2022. Vol. 359. No. 3. P. 1382-1406.
14. Miranda-Colorado, R. & Aguilar, L. A family of anti-swing motion controllers for 2D-cranes with load hoisting/lowering. *Mechanical Systems and Signal Processing.* 2019. Vol. 133. No. 106253.
15. Hrabovský, L. & Cepica, D. & Frydrýšek, K. Detection of mechanical stress in the steel structure of a bridge crane. *Theoretical and Applied Mechanics Letters*. 2021. DOI: https://doi.org/10.1016/j.taml.2021.100299.
16. Shumei, M. & Ran, T. & Liyun, X. & Liangsheng, Y. Delivery operation time optimization of multi-crane scheduling in steel plate yard. In: *Procedia CIRP.* 2021. Vol. 104. P. 1077-1082.
17. Huang, C. & Li, W. & Lu, W. & Xue, F. & Liu, M. & Liu, Z. Optimization of multiple-crane service schedules in overlapping areas through consideration of transportation efficiency and operational safety. *Automation in Construction.* 2021. Vol. 127. No. 103716.
18. Hu, S. & Fang, Y. & Guo, H. A practicality and safety-oriented approach for path planning in crane lifts. *Automation in Construction.* 2021. Vol. 127. No. 103695.
19. Price, L. & Chen, J. & Park, J. & Cho, Y. Multisensor-driven real-time crane monitoring system for blind lift operations: Lessons learned from a case study. *Automation in Construction.* 2021. Vol. 124. No. 103552.
20. Eberharter, J. & Rajek, M. Dynamic Anti-Collision System for Hydraulic Cranes. In: *Proceedings of the 18th World Congress*. The International Federation of Automatic Control. Milano (Italy) August 28 - September 2, 2011.
21. Hwang, S. Ultra-wide band technology experiments for real-time prevention of tower crane collisions. *Automation in Construction.* 2012. Vol. 22. P. 545-553.
22. Margielewicz, J. & Haniszewski, T. & Gąska, D. & Pypno C. *Badania modelowe mechanizmów podnoszenia suwnic*. Katowice: Polish Academy of Science. 2013. 204 p. [In Polish: *Model studies of cranes hoisting mechanisms*].
23. Matyja, T. Safety of transport operations performed using pallet load units. *Scientific Journal of Silesian University of Technology. Series Transport*. 2021. Vol. 112. P. 145-156.
24. Autodesk Inventor – Software Help Files. Available at: https://knowledge.autodesk.com; https://www.autodesk.com/2018.06.04.

Received 25.03.2021; accepted in revised form 25.08.2022